The Fluid Mechanics of Slag-Metal Interactions in Ladle Metallurgy

*Krishnakumar KRISHNAPISHARODY and Gordon A. IRONS**
Steel Research Centre, McMaster University, Hamilton, ON, Canada

Abstract: In Ladle Metallurgy operations following steelmaking, the control of the interactions between slag and metal is crucial for the production of high-quality steel. While the chemical aspects of the refining have been well studied, the fluid dynamic aspects have received less attention. Ladles are often gas-stirred by porous plugs pushing the slag to the periphery of the ladle and opening "eyes" of steel exposed to the atmosphere. The nominal slag-metal contact area is reduced, but there may be entrainment of slag in metal and *vice versa* which increases the effective interfacial area. Experiments were conducted with water models and the work of others in metallic systems has been included in the study. The eye size has been found to be quite different for thin and thick slag layers, and mathematical models of the controlling factors for the eye size has been determined for these two regimes. The models show that the important factor is the balance between the inertia from the gas-liquid plume and height of the slag, so the governing equations are based on Froude number control. The conditions for closure of the eye have been identified and mathematically modeled. At higher gas flow rate, droplets of slag are entrained into metal which is quantitatively linked to Kelvin-Helmholtz instability. The role that physical properties of the slag play in these phenomena is discussed.

Key words: Steelmaking, fluid mechanics, Kelvin-Helmholtz instability, bubbles, droplets

1. Introduction

In a gas-stirred ladle, the upward flow inside the two-phase plume creates a dome-shaped region directly above the bubble plume. This elevated region of the bath surface is usually called the "spout". If there is a slag layer present above the metal, it is pushed towards the sides, leaving an exposed metal surface usually called the "slag eye". These phenomena are important in Ladle Metallurgy due to factors such as: (i) Oxygen and Nitrogen pick-up at the exposed spout and eye regions which lead to the deterioration of steel quality (ii) the formation of slag droplets at the periphery of the eye resulting in slag-metal mixing and (iii) the refining reactions with the slag are limited to the slag-metal contact area. Thus, a better understanding of the characteristics of these regions is necessary for the control and optimization of ladle processing operations aimed at producing steels of high quality. In the present paper, the factors governing the size of the eye will be examined, and mathematical models presented. Work was also conducted on the conditions for the formation of slag droplets that may be entrained in the steel.

2. Eye Size for Thin Slag

A mechanistic model has been developed so that eye size can be calculated as a function of gas flow rate and the heights of the upper and lower phases [1]. As will be shown, there is good agreement with the present experimental results, and those of others; therefore, the model will be useful for Ladle Metallurgy applications. In these applications,

the slag layer is relatively thin (where the height-to-metal height, h/H, is usually less than 0.1), and can be pushed aside relatively easily. The work was conducted with water and oil to simulate the steel and slag, respectively. A photograph of the eye obtained under such conditions is shown in Figure 1.

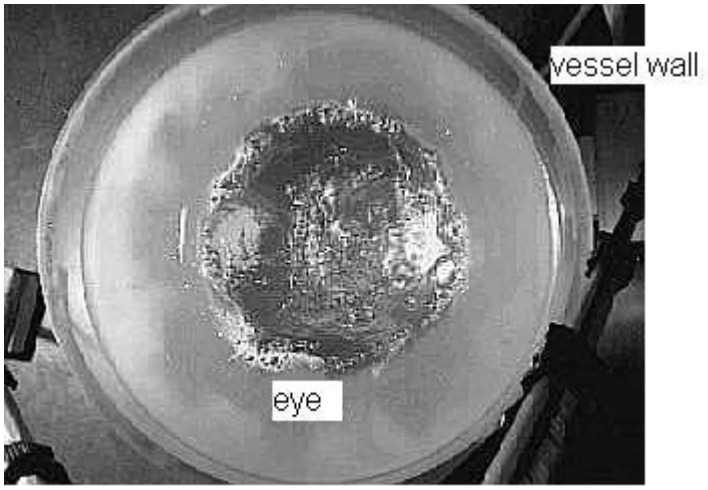

Fig. 1. A photograph from the top of the eye in a 1/10-scale water model; water and oil simulate the steel and slag, respectively (42 cm bath height, 1 cm oil height, and 2 l/min gas flow rate). The injected gas rises in the center, and the oil is pushed to the periphery. There is some mixing of the oil and water at the boundary.

Referring to Figure 2, AA'D'D is a section of the eye, which is larger than the spout zone. Without gas bubbling, the water resides below the oil due to the density difference. The gas bubbling creates an upward momentum flux of gas and liquid across BB' supporting the water column and the spout above it. Similarly, the downward flow across AB supports the donut-shaped water column above it. The toroid outside the plume region is selected as the control volume for the force balance.

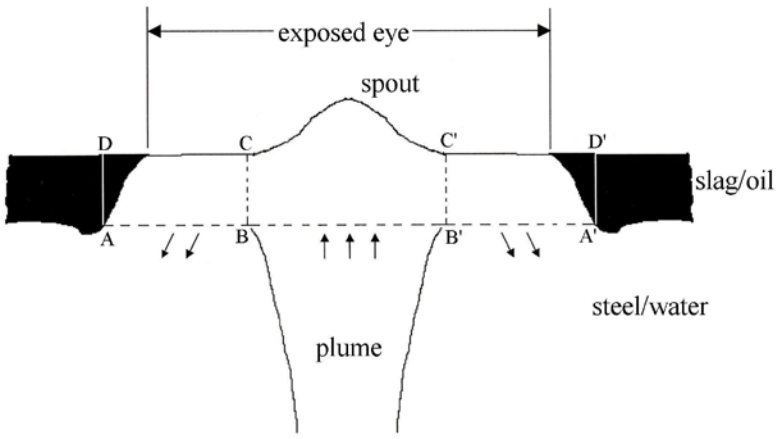

Fig. 2. Schematic diagram of the eye formation process for thin top layers

A linear momentum balance over a representative section of the toroid, ABCD, is performed by considering the various forces acting on it, as shown in Figure 3. In this analysis h is the height of the top layer, W is the weight of the water mass, and p_a and p_b are the pressures at the top and bottom of the control volume, respectively. The upward plume velocity across BB' is U_p, whereas U_0 is the velocity of bottom layer flow crossing AB. Experimental observation revealed that the water-oil interface has a bell-shaped contour as shown in Figure 2 and that the downward flow is directed at an angle θ to the vertical, as indicated in Figure 3.

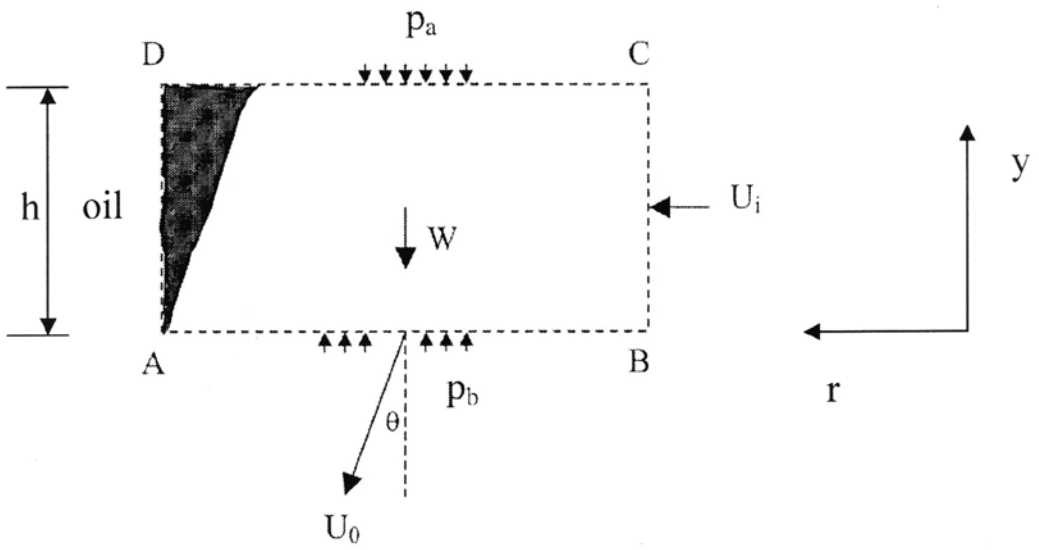

Fig. 3. Control volume for momentum balance.

It is assumed that section BC corresponds to the plume boundary and the flow into the control volume at this section is horizontal. Further, the velocity across section AB is assumed to be uniform. With these assumptions, a linear momentum balance in the vertical (y) direction over the section ABCD, yields the following relationship:

$$p_b A\mathbf{j} - p_a A\mathbf{j} - W\mathbf{j} - \iint_A \rho v(\mathbf{V}\bullet\hat{\mathbf{n}})\,dA = 0 \tag{1}$$

where A is the area of the section AB, v is the y-component of velocity vector and **j** is the unit vector in the y direction.

After some manipulation, the eye size is related to the plume size:

$$\frac{A_e}{A_p} = a + b\left(\frac{\rho}{\Delta\rho}\frac{U_p^2}{gh}\right)^{1/2} \tag{2}$$

where a and b are constants.

Figure 4 shows all available data put into a form to evaluate Equation (2). The straight line behavior demonstrates that it is consistent with the data over a wide range of conditions, and the slope and intercept of the line are shown on the Figure.

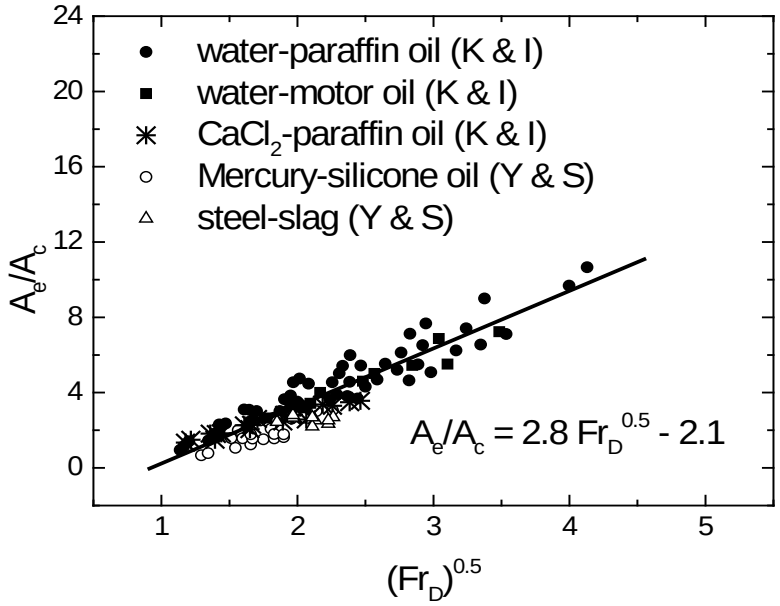

Fig. 4. Variation of non-dimensional eye area as in Eq. (2) with the square root of the densimetric Froude number (K & I: Krishnapisharody and Irons[1], Y & S: Yonezawa and Schwerdtfeger[2]).

3. Eye Size for Thick Slags

In this section, the mechanistic-based approach developed in the previous section has been extended to the case of ladle processing with a thick slag layer [3]. If the slag layer is sufficiently thick, the eyes formed are smaller than the spout region. The eye formation process under such configuration is schematically shown in Figure 5. Generally, h/H is greater than 0.1.

The situation for eye formation in thick slag is shown schematically in Figure 5. Unconfined gas-liquid bubble plumes are observed to expand in a nearly conical fashion. When the plume reaches within a short distance of the bath surface, of the order of the plume radius, it expands and flows radially. In this region, the predominantly upward flow develops radial velocity components. This turning flow drives the top layer to the side thereby creating the ‘eye’. At the periphery of the eye region, the radial flow is diverted downward. The inertial effects of the upward flow in the central plume region as well as of the downward flow from the region close to the oil-water interface support the denser column of water in the lighter oil phase. Thus, as in the previous case, an analysis of various forces acting on this region by means of a control-volume approach will elucidate the process of eye formation.

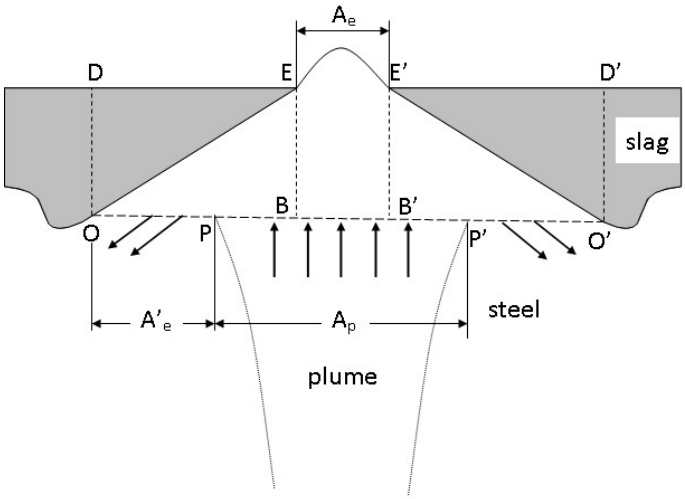

Fig. 5. Schematic representation of the eye formation process for thick top layers.

A linear momentum balance over the section OBED in Figure 5 is performed by considering the various forces acting on this control volume, as shown in Figure 6. U_p is the upward plume velocity across PP' and U_0 is the downward velocity of the turning flow across OP. In actual practice, the water-oil interface takes the form of a bell-shaped contour as shown in Figure 1 and the downward flow is directed at an angle θ to the vertical.

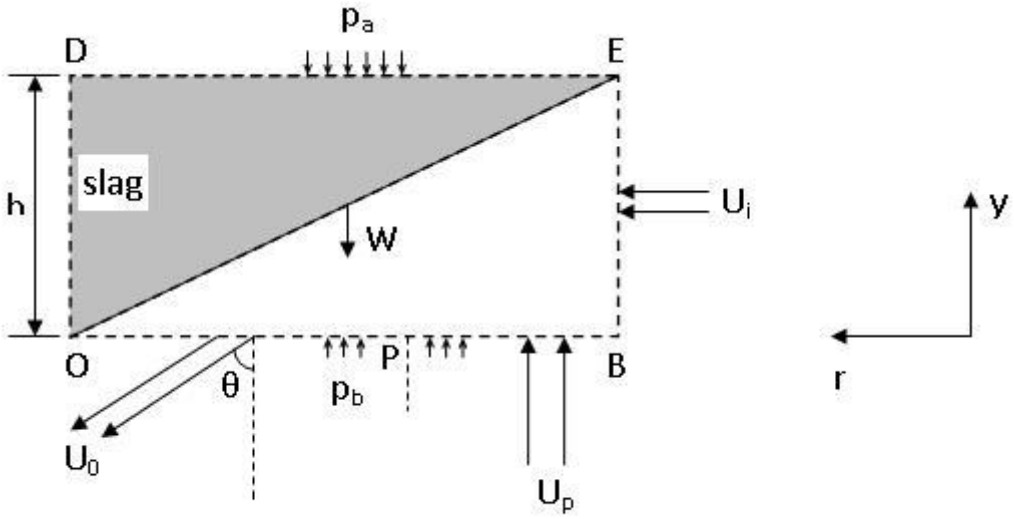

Fig. 6. Control volume for linear momentum balance.

With similar assumptions as in the previous section, the linear momentum balance in the y-direction over the section OBED is:

$$p_b A j - p_a A j - W\,\mathbf{j} - \iint_A \rho v(\mathbf{V}\bullet\hat{\mathbf{n}})\,dA = 0 \tag{3}$$

where A is the area of the section OB, *v* is the y-component of velocity vector and **j** is the unit vector in the y direction. The above equation can be expressed in the form:

$$\left(a - \frac{A_e}{A_p}\right)\rho U_p^2 = b\,\Delta\rho\, gh \tag{4}$$

where *a* and *b* are numerical constants. Equation (4) can be further manipulated to:

$$A^* = \frac{A_e}{A_p} = a - \left(\frac{\Delta\rho}{\rho}\right)\frac{b}{Fr} \tag{5a}$$

$$A^* = \frac{A_e}{A_p} = a - \frac{b}{Fr_D} \tag{5b}$$

Thus, the dimensionless eye area A_e/A_p is a function of the Froude number U_p^2/gh and the density ratio of the liquids, where the Froude number is based on the height of the top layer (slag). Therefore, the eye size for thick slag depends on the same variables as for thin slag (Eq. (2)).

There is less data available on the eye sizes for thick slag layers, which is plotted in Figure 7 to determine if the data conforms to Equation 13b. Again, there is good agreement with available experimental evidence.

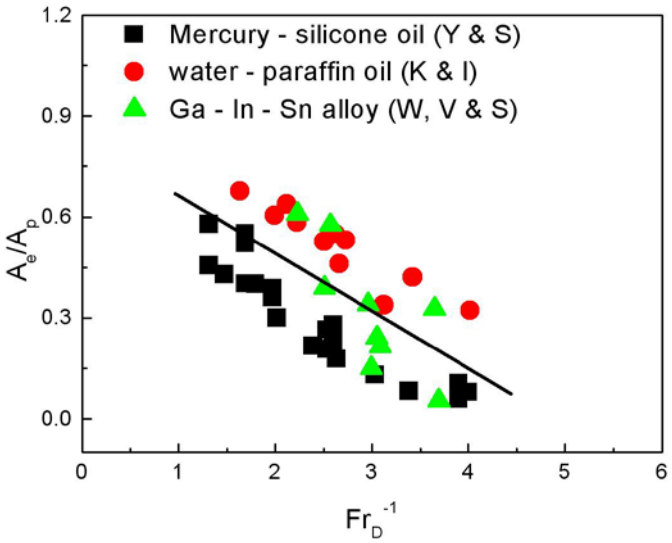

Fig. 7. Variation of the dimensionless eye area with the densimetric Froude number as in Eq. (5b). The data were taken from Yonezawa and Schwerdtfeger [2] (Y &S), Krishnapisharody and Irons [3] (K & I) and Wu *et al.* [4] (W, V and S).

3.1 Critical Gas Flow Rates for Slag Eye Opening

Another parameter of interest in Ladle Metallurgy is the critical gas flow rate for soft bubbling of Argon below which no eye opens. In these conditions the gas passes through the slag as individual bubbles with insufficient momentum to open the eye. The condition can obtained by setting Equation (5b) to zero and rearranging for the critical value of Fr_D:

$$Fr_D = \frac{\rho}{\Delta\rho}\frac{U_p^2}{gh} = 0.203 \tag{6}$$

The average plume velocity at the top level of the plume is taken from the correlation of Krishnapisharody and Irons:[5]

$$U_p = 2.57 Q^{0.32} H^{-0.28} \tag{7}$$

Using Equations (7) and (7), the critical gas flow rate required to open the slag eye is:

$$Q_c = 0.0035\left[\left(\Delta\rho/\rho\right) g h\right]^{3/2} H^{0.84} \tag{8}$$

This model is applied to predict the critical gas flow rates in two different systems and the results are shown as a scatter plot in Figure 8. The values in Figure 8 are representative of a range of experimental conditions. It can be seen that most of the observed values fall within $\pm$ 40 % of the predictions.

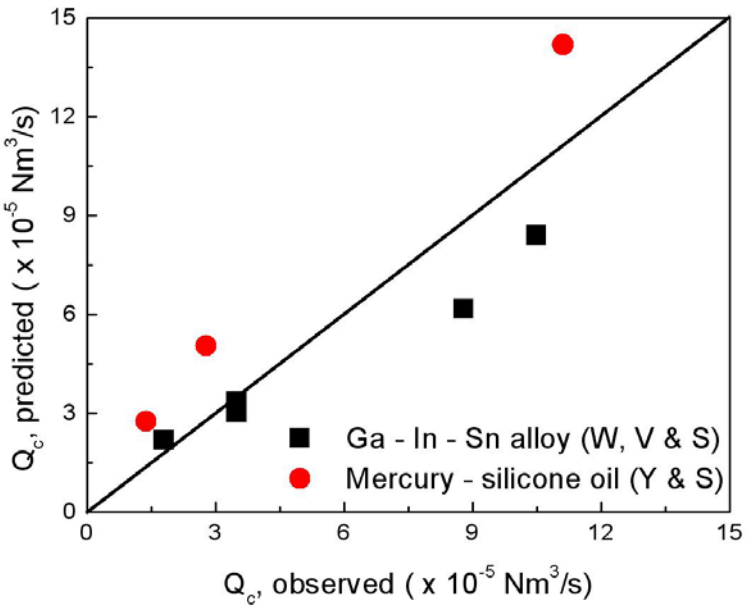

Fig. 8. Comparison of the observed and predicted critical gas flow rates for the generation of open eyes. The data were taken from Yonezawa and Schwerdtfeger [2] (Y &S) and Wu *et al.* [4] (W, V and S).

Finally, to illustrate the application of this model in full-scale systems, similar calculations have been performed for a 300 tonne steel-slag system with the following assumed parameters: density of steel = 7000 kg/m^3, density of slag = 3000 kg/m^3, steel height = 3m and slag height = 5 – 10 cm. The critical gas flow rates were obtained in the range 1.5 – 3.5 Nm^3/hr. This is in fair agreement with the observations of Wu *et al*.[4] in a similar industrial ladle, where eyes were found to open when the flow rate reached 1 – 2 Nm^3/hr under a slag cover of about 4 – 8 cm.

4. Slag Entrainment Modelling

It has been known for some time that slag in ladles can become entrained in the metal, and that this contributes to higher rates of slag-metal refining because of the greater interfacial area. The conditions for the onset of the entrainment have not been adequately clarified, so work with a water-oil model [6] and mathematical modelling [7] has been conducted.

4.1 Oil-Water Thin Slice Model

The study of the dynamics of the liquid-liquid interface and velocity distributions on both sides of the interface requires tracking the development contours of the interface in real-time and measuring the velocity fields in the two-fluid system. These measurements are not easily accomplished in a cylindrical model system due to image distortions arising from curvature effects. As a result, it was decided to construct a rectangular thin-slice model in which the interface positions and liquid velocities can be easily measured in a vertical plane.

The model was designed to have a circulatory flow pattern similar to a gas-stirred ladle. In gas-stirring, the injection of the gas through the bottom creates circulation of the bulk liquid (water). However, the inherent instability of the two-phase plume makes the water-oil interface to oscillate violently. In order to make the jet flow and thereby the interface more stable in the model, the stirring was created by issuing a water jet into the water bath. To maintain the bath level, the water was circulated in a closed loop with a pump.

The thin-slice model, shown in Figure 9, is a rectangular cavity made of transparent acrylic and consists of an upper flow chamber and a lower circulation chamber. Water enters the flow chamber through a narrow slot of 0.5 cm thickness at the centre and exits through sections 10 times wider than the inlet on either side of the chamber. This arrangement ensures a plane velocity comparable to gas-stirred ladles, but with a gentle circulation at the sides. To maintain a two-dimensional character to the flow without excessive wall effects at the central plane, the thickness of the chamber was selected as 5 cm after assessing the influence of boundary layers.

Simultaneous measurements of velocities near the interface in both the fluids have been performed using the Particle Image Velocimetry (PIV) technique. The technique also permitted photographic capture of the events at the interface.

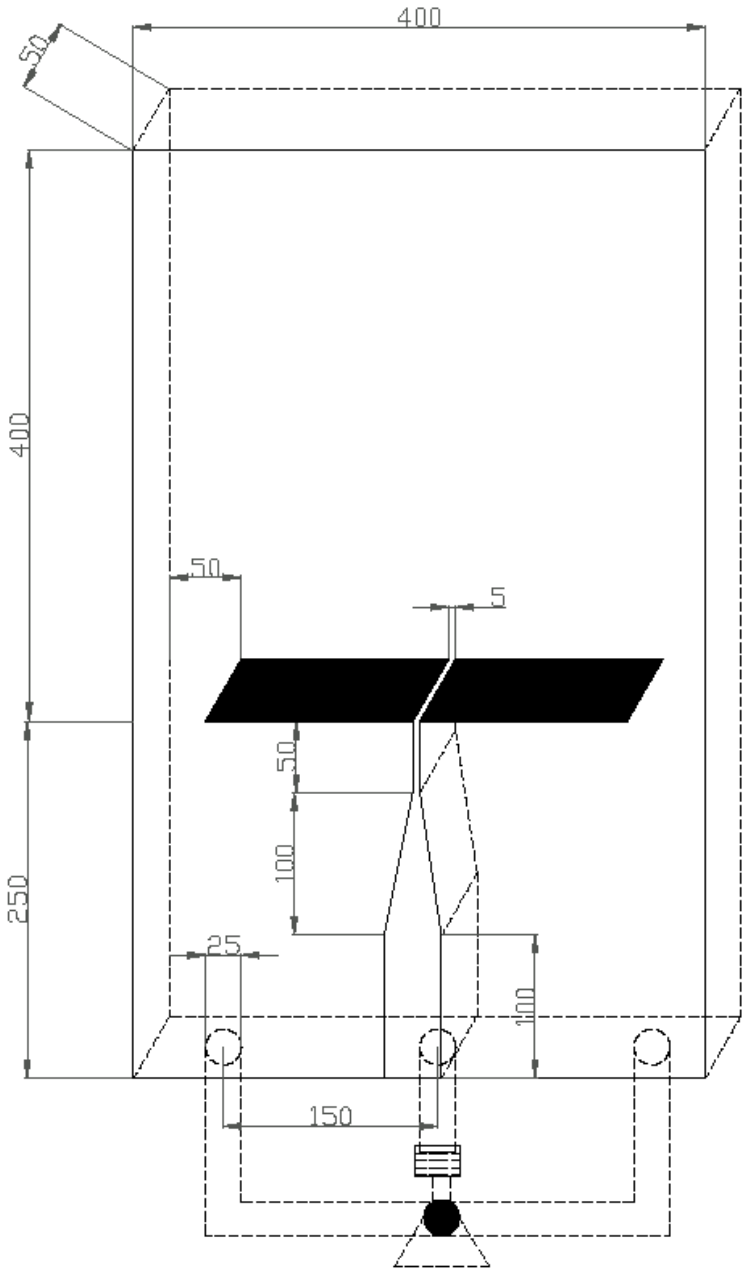

ALL DIMENSIONS IN MM; P – Pump, R - Rotameter

Fig. 9. Schematic diagram of the experimental apparatus.

Figures 10(a) and (b) show the interface locations in the water-paraffin oil system for two different inlet jet velocities of 0.47 and 0.67 m/s, respectively. Since the water jet is symmetric, the flow in the chamber is the same on either side of the jet axis, so these figures show only the left side of the chamber. The right border in these figures is the axis of the jet.

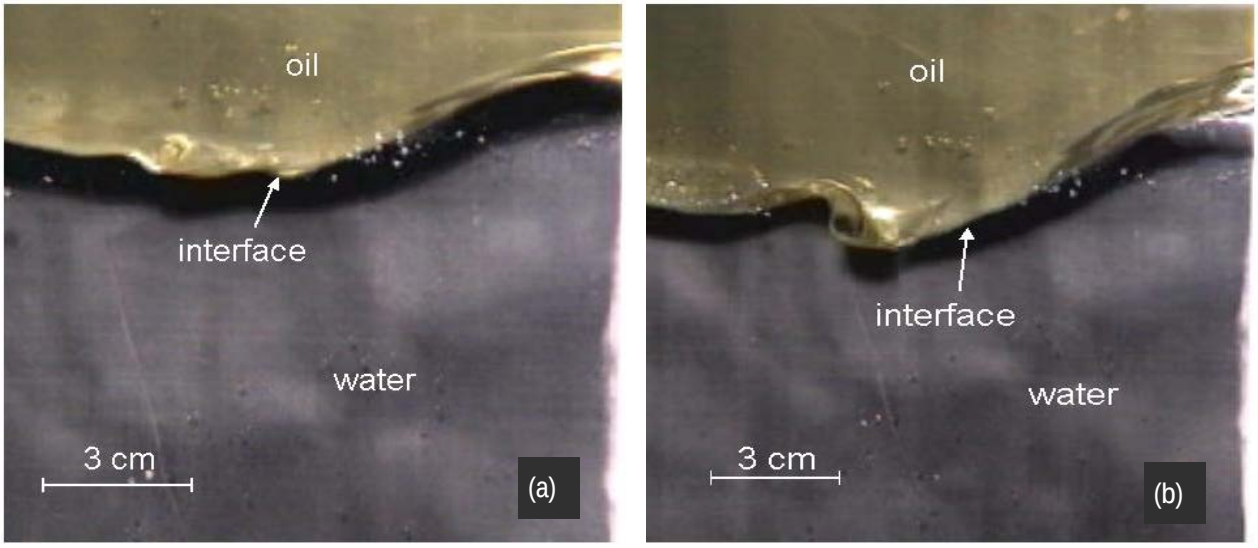

Fig. 10. Interface positions in the water-paraffin oil system illustrating (a) lip formation and (b) ligament formation.

Three distinct stages were observed in the evolution of the water-oil interface in the formation of oil droplets:

1. Formation of a lip at the trough of the interface
2. Growth of the lip into a ligament
3. Break-up of the ligament into smaller droplets

Instability of the Kelvin-Helmholtz type was investigated as the most probable mechanism, due to the nature of the flow configuration. Kelvin-Helmholtz instability arises when two stratified fluids have relative motion. For the horizontal flow of two incompressible inviscid fluids, the Kelvin-Helmholtz instability criterion is expressed in terms of a critical velocity difference between the fluids as [8]:

$$\Delta U_c^2 = \left(\frac{\rho_1 + \rho_2}{\rho_1 \rho_2}\right)\left[(\rho_1 - \rho_2)\frac{g}{k} + \sigma k\right] \tag{9}$$

Where ΔU_c is the critical velocity difference, ρ_1 and ρ_2 are the densities of the denser and lighter liquids, respectively, g is the gravity constant, σ is the interfacial tension and k is the wave number. ΔU_c is a function of the wave number, and consequently, the instability depends on the wave number, k. The wave number at the minimum ΔU_c is [8]:

$$k = \sqrt{\frac{g(\rho_1 - \rho_2)}{\sigma}} \tag{10}$$

From Equations (9) and (10), the minimum value of the critical velocity difference is:

$$\Delta U_c^2 = \frac{2(\rho_1 + \rho_2)}{\rho_1 \rho_2} \sqrt{\sigma g (\rho_1 - \rho_2)} \tag{11}$$

For the water-paraffin oil system used in the present study, the critical velocity difference obtained by applying Equation (11) is about 0.19 m/s. Considering an order of magnitude difference, the bulk velocities inside the water layer has to be about 0.21 m/s, close to the experimentally measured value of 0.26 m/s. These observations imply that the Kelvin-Helmholtz instability is the dominant mechanism leading to the droplet formation in the water-oil system. Iguchi *et al.* [9] also observed a critical velocity difference of about 0.2 m/s in systems of salt water and various silicone oils for a different flow configuration. They created the flow around the interface by tilting the apparatus through an angle.

4.2 Mathematical Modelling

For this work, the Volume-of-Fluid (VOF) Method was used for the modeling. The VOF model is a fixed grid technique designed to capture the interface between two or more immiscible fluids [10]. In this method, the interface is not tracked directly; instead, the model tracks a VOF function advected with the fluid, which represents the volume fraction (*F*) of a given fluid in any cell of interest. By solving a separate conservation equation for the *F* function, the interface is reconstructed from the distribution of *F* in the domain.

In the SIMPLE-VOF method, a single set of momentum equations is shared by the fluids and the volume fraction of each of the fluids in every cell is tracked throughout the computational domain *via* the *F* function. The governing equations of the model are continuity, momentum and conservation of the VOF function (*F*). In vector notation, the governing equations are:

$$\nabla . \boldsymbol{U} = 0 \tag{12}$$

$$\frac{\partial(\rho \boldsymbol{U})}{\partial t} + \nabla . (\rho \boldsymbol{U}\boldsymbol{U}) = -\nabla p + \nabla . \tau + \boldsymbol{F_b} \tag{13}$$

$$\frac{\partial F}{\partial t} + \nabla . (\boldsymbol{U} F) = 0 \tag{14}$$

where $\boldsymbol{U}$ is the velocity vector, τ is the shear stress tensor, ρ is the density, p is the pressure and $\boldsymbol{F_b}$ is the body force. The details of the implementation of the model have been previously described [7].

The results of the modelling are compared with the thin-slice photographs in the following two figures with a time sequence of a single droplet formation. The agreement is reasonably good in the shape of the interface and the frequency of droplet formation. However, the droplet size is somewhat smaller than in the experiments.

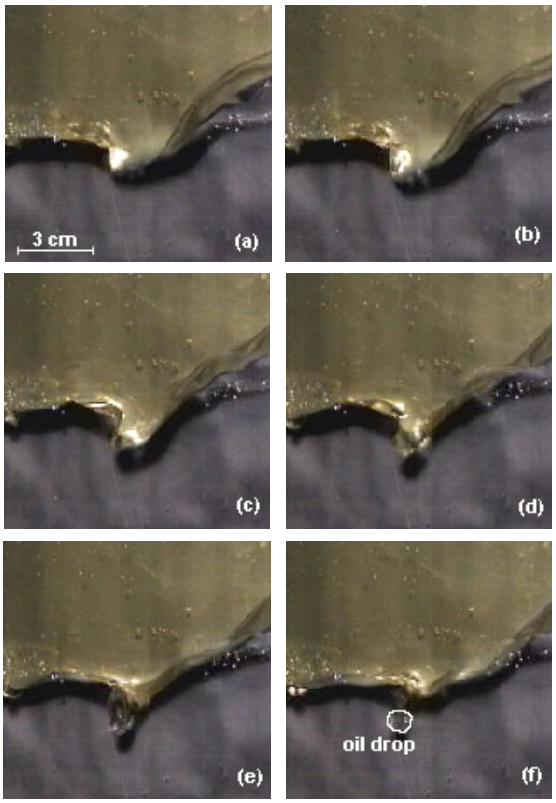

Fig. 11. A series of video pictures showing the processes leading to droplet generation, for the water-paraffin oil system. The time interval between the frames is 66.7 ms.

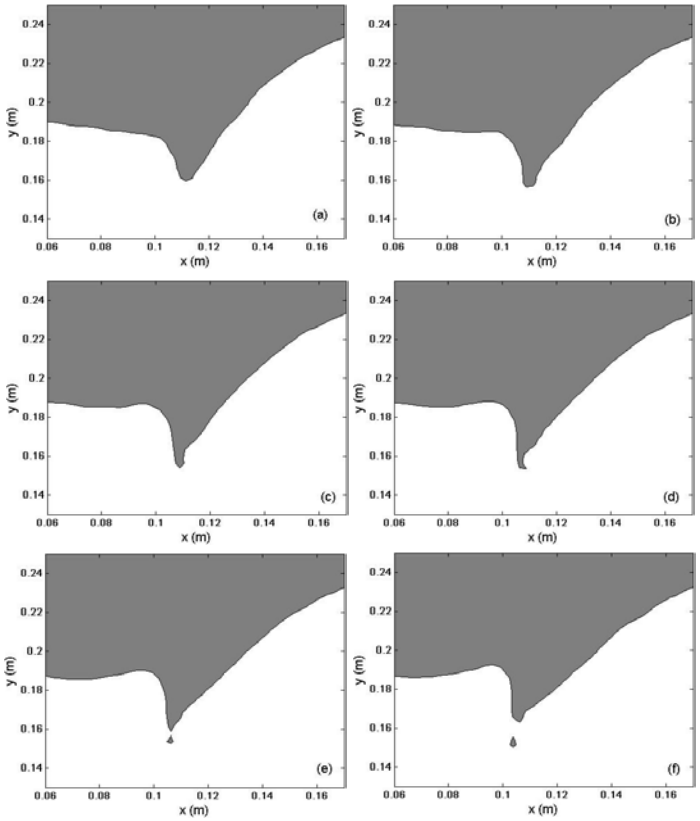

Fig. 12. Numerical simulation of droplet formation. Frame (a) is obtained at t = 1.9 s from the start of simulation; other frames are sequentially separated by a time interval of 67 ms.

5. Discussion

The eye sizes for both the thin and thick slag conditions were well described as functions of Froude numbers. This finding coupled with the derivation of the governing equations shows that the force balance controlling the eye size is based on the inertia of the plume working against the buoyancy of the slag relative to the metal. Experiments were conducted with different oils to see the effects of other physical properties of the oil, simulating the slag phase. It was found that higher viscosity oils had the same eye size, but it took a few seconds longer for the eye to form. Thus, the viscous dissipation forces are relatively small. The difference in surface tension had a small effect because the amount of new interface created to form an eye was small.

The waves generated in the entrainment experiments were in the intermediate region between gravity waves and capillary waves so that the wave number and the critical velocity depended on both the density difference and the interfacial tension, as shown by Equation 11. There was also a minor effect of the viscosity of the slag on the critical velocity.

6. Conclusions

In this paper the conditions for the formation of slag eyes in both thin and thick slags have been presented in a form that can easily be used by those in steel plants. The eye size is controlled by a force balance between the inertia of the rising gas-steel plume and the density difference between the slag and metal. In the thick slag case, the eye can close at low flow rates, so that individual bubbles rise through the plume. The conditions for eye closure have been determined. The onset of entrainment of the upper phase into the lower phase has been determined with a thin-slice water and oil model and a mathematical model. The formation of the droplets follows the classical interface instability leading to ligaments and finally the creation of separate droplets. The velocity for the onset of entrainment is consistent with Kelvin-Helmholtz instability.

References

[1] K. Krishnapisharody and G.A Irons. Modeling of Slag Eye Formation over a Metal Bath Due to Gas Bubbling, *Metall. Mater. Trans. B*, 2006, 37B, p. 763-772.

[2] K. Yonezawa and K. Schwerdtfeger. Spout Eyes Formed by an Emerging Gas Plume at the Surface of a Slag-Covered Metal Melt, *Metall. Mater. Trans. B*, 1999, Vol. 30B, 1999, p. 411-418.

[3] K. Krishnapisharody and G.A. Irons. A Model for Slag Eyes in Steel Refining Ladles Covered with Thick Slag, *AISTech2011 Proceeding*, 2011, Volume II, p. 463-472.

[4] L. Wu, P. Valentin and D. Sichen. Study of Open Eye Formation in an Argon Stirred Ladle. *Steel Res. Int.*, 2010, 81, 7, p. 508-515.

[5] K. Krishnapisharody and G. A. Irons. A Study of Spouts on Bath Surfaces from Gas Bubbling: Part II. Elucidation of Plume Dynamics. *Metall. Mater. Trans. B*, 2007, 38B, p. 377-388.

[6] K. Krishnapisharody and G.A. Irons. Model Studies of Slag Droplet Generation in Gas Stirred Ladles. *Materials Processing Fundamentals*, 2008, TMS, p. 293 - 302.

[7] K. Krishnapisharody and G.A. Irons. Numerical Simulation of Droplet Generation of the Buoyant Phase in Two-Phase Liquid Baths. *Materials Processing Fundamentals*, 2008, TMS, p. 311 - 321.

[8] S. Chandrasekhar. Hydrodynamic and Hydromagnetic Stability, Dover Publications Inc., New York, 1961.

[9] M. Iguchi, J. Yoshida, T. Shimizu and Y. Mizuno. Model Study on the Entrapment of Mold Powder into Molten Steel. *Iron Steel Inst. Jpn. Int.*, 2000, 40, p. 685-691.

[10] C.W. Hirt, and B.D. Nichols. Volume of Fluid Method for the Dynamics of Free Boundaries. *Journal of Computational Physics*, 1981, 39, p. 201-225.